Journal of Organometallic Chemistry 852 (2017) 34–42

Contents lists available at ScienceDirect

Journal of Organometallic Chemistry

journal homepage: www.elsevier.com/locate/jorganchem

New iron cyclopentadienyl complexes bearing different phosphane *co*-ligands: Structural factors *vs.* cytotoxicity

Adhan Pilon [a, 1], Patrícia Gírio [a, 1], Guilherme Nogueira [a], Fernando Avecilla [b], Harry Adams [c], Julia Lorenzo [d], M. Helena Garcia [a, **], Andreia Valente [a, *]

[a] Centro de Química Estrutural, Faculdade de Ciências da Universidade de Lisboa, Campo Grande, 1749-016 Lisboa, Portugal
[b] Grupo Xenomar, Centro de Investigacións Científicas Avanzadas (CICA), Departamento de Química, Facultade de Ciencias, Universidade da Coruña, Campus de A Coruña, 15071 A Coruña, Spain
[c] Department of Chemistry, University of Sheffield, Sheffield S3 7HF, UK
[d] Institut de Biotecnologia i de Biomedicina, Departament de Bioquímica i Biologia Molecular, Universitat Autònoma de Barcelona, 08193 Bellaterra, Barcelona, Spain

ARTICLE INFO

Article history:
Received 18 August 2017
Received in revised form
3 October 2017
Accepted 5 October 2017
Available online 7 October 2017

Keywords:
Iron cyclopentadienyl
Electronic flow
Anticancer
Apoptosis

ABSTRACT

A new family of piano stool iron-cyclopentadienyl compounds bearing different phosphane co-ligands has been synthesized. All the compounds, with the general structure $[Fe(Cp)(CO)(PR_3)(L)]^n$ (PR_3 = triphenylphosphane, 4-(diphenylphosphino) benzoic acid or tris(4-fluorophenyl)phosphane; when L = I, n = 0; when L = 4-aminobenzonitrile, n = +1) were fully characterized by the usual analytical and spectroscopic techniques. Interestingly, compound $[Fe(Cp)(CO)(PPh_3)I]$ **1** crystalizes in the orthorhombic space group $P2_12_12_1$ and its crystal packing only contains one enantiomer, while compound $[Fe(\eta^5\text{-}Cp)(CO)(P(Ph\text{-}p\text{-}F)_3)I]$ **3** crystalizes in the centrosymmetric space group *Pbca* presenting an important disorder in the structure, probably due to the presence of the two enatiomers in the crystal packing. All the compounds presented adequate stability in aqueous solution and they were tested against cervical HeLa human cancer cells. The cationic complexes bearing triphenylphosphane (**4**) or tris(4-fluorophenyl)phosphane (**6**) were found to be highly cytotoxic, causing cell death by apoptosis. The results point out that the electronic features of the new compounds might be related to their cytotoxic activity.

1. Introduction

Iron is a biometal essential for human life being a building element in several important proteins [1]. Its presence in many biological functions, importance in cell replication, metabolism and growth, along with the anticancer properties already shown for some iron complexes, makes it an appealing candidate to be used in anticancer drugs. Indeed, the discovery [2] and structural characterization [3] of the "sandwich" compound ferrocene, in the early 1950s and the pioneer work of Köpf and Köpf-Maier discovering the cytotoxic properties [4,5] of ferrocenium, the oxidized form of ferrocene, paved the way for the search of iron compounds to be used in cancer therapy. In this frame, the search for new iron compounds with anticancer properties has been essentially focused on ferrocene derivatives [6]. Ferrocene by itself is not a particularly cytotoxic compound [7]. However, ferrocifens, derivatives of tamoxifen (a chemotherapeutic agent for patients with hormone-dependent breast cancer), revealed anticancer activity against hormone-dependent (MCF7) and independent (MDA-MB-231) breast cancer cell lines [8–10]. Ferrocene derivatives suffer, however, from bioavailability problems, restricting them from entering into clinical studies [7].

The encouraging results obtained by our group with piano stool structured compounds based on the "RuCp" fragment (Cp = η^5-C_5H_5) [11–18] together with the success found for ferrocene derivatives lead us to enlarge our work to the compounds with "FeCp" bearing a half-sandwich geometry. We have recently published our results concerning two new families of organometallic iron compounds based on the general cationic structure $[Fe(Cp)(dppe)(L)]^+$, where dppe = ethylenebis(diphenylphosphane) and L = imidazole

* Corresponding author.
** Corresponding author.
E-mail addresses: mhgarcia@fc.ul.pt (M.H. Garcia), amvalente@fc.ul.pt (A. Valente).
[1] These authors contributed equally to this work.

https://doi.org/10.1016/j.jorganchem.2017.10.004
0022-328X/

based ligands [19] or nitrile ligands [20]. These two new families showed cytotoxicity against breast MCF7 [19], cervical HeLa [19], ovarian A2780[19] and leukemia HL-60[20] human cancer cells lower than those found for cisplatin in the same experimental conditions. Other complexes bearing the "FeCp" scaffold and bearing nitrile carbohydrate derivative ligands also showed good cytotoxicities against a colon cancer cell line (HCT116) [21].

Complexes $[FeCp(CO)_2X]$ (X = halide, NCS, BF_4^-) and $[FeCp(CO)_2]_2$ showed cytotoxicity towards MDA-MB-231 breast and HeLa cervical cancer cells (IC_{50} = 3.0–17.3 μM, 24 h incubation), while being non-cytotoxic towards normal mammary epithelial cells MCF-10A [22].

In this study, we have decided to explore the simultaneous effect of different σ donor phosphane ligands with the π acceptor character of the carbonyl co-ligand, that might tune the complex cytotoxicity [16]. The competitive π acceptor effect of the benzonitrile derivative ligand is expected to impart strong electronic effects on the iron complexes due to its involvement in strong metal-ligand π-backdonation via the d metal-π* NC orbitals [23].

2. Experimental section

2.1. General procedures

All reactions and manipulations were performed under nitrogen atmosphere using *Schlenk* techniques. All solvents used were dried and freshly distilled under nitrogen prior to use, using standard methods [24]. ^1H, ^{13}C and ^{31}P NMR spectra were recorded on a Bruker Avance 400 spectrometer at probe temperature using commercially available deuterated solvents. ^1H and ^{13}C chemical shifts (s = singlet; d = duplet; t = triplet; m = multiplet; comp = complex) are reported in parts per million (ppm) downfield from internal standard Me_4Si and the ^{31}P NMR spectra are reported in ppm downfield from external standard, 85% H_3PO_4. Coupling constants are reported in Hz. All assignments were attributed using ^{13}C APT or DEPT-135, COSY, HMBC, HSQC and HMQC NMR techniques. Infrared spectra were recorded on KBr pellets using a Mattson Satellite FT-IR spectrophotometer. Only considered relevant bands were cited in the text. Electronic spectra were obtained at room temperature on a Jasco V-560 spectrometer from solutions of 10^{-3}-10^{-5} M in quartz cuvettes (1 cm optical path). Elemental analyses were performed at *Laboratório de Análises*, at *Instituto Superior Técnico*, using a Fisons Instruments EA1 108 system. Data acquisition, integration and handling were performed using a PC with the software package EAGER-200 (Carlo Erba Instruments).

2.2. Synthesis

The starting material $[Fe(\eta^5\text{-}Cp)(CO)_2I]$ was prepared from the commercially available dimer $[Fe(\eta^5\text{-}Cp)(CO)_2]_2$ following the literature procedure [25].

2.3. General procedure for the synthesis of $[Fe(\eta^5\text{-}Cp)(CO)(PR_3)I]$ complexes **1**-**3**

To a stirred and degassed solution of $[Fe(\eta^5\text{-}Cp)(CO)_2I]$ (1 mmol) in dry acetone (30 mL) PR_3 (1 mmol) was added. The reaction mixture was then irradiated under UV light (125 W) for 3–7 h (see below). The precipitate was separated by cannula-filtration and the solvent was evaporated under vacuum. The residue was twice recrystallized from dry dichloromethane/*n*-hexane and dark green products are obtained.

$[Fe(\eta^5\text{-}Cp)(CO)(PPh_3)I]$ **1**

Yield: 69% (371 mg; 0.69 mmol). Irradiation time: 4 h. Microcrystalline green powder. Single crystals for X-ray diffraction studies were obtained by crystallization from THF/*n*-hexane solution. IR (KBr, cm^{-1}): ν(C-H aromatics) 3047, ν(C≡O) 1936, ν(C-C aromatics) 1473, 1427. ^1H NMR (DMSO-d_6, Me_4Si, δ/ppm): 7.47 (comp, 15, H_2+H_3+H_4); 4.59 (s, 5, Cp). ^{13}C NMR (DMSO-d_6, Me_4Si, δ/ppm): 221.40 (d, J_{CP} = 31.2, C≡O); 135.34 (d, $^1J_{CP}$ = 43.5, C1); 133.15 + 128.28 (d, J_{CP} = 9.4; d, J_{CP} = 9.6, C3 + C2); 130.21 (C4); 82.93 (Cp). ^{31}P NMR (DMSO-d_6, δ/ppm): 67.04 (s). UV–Vis in DMSO, λ_{max}/nm (ε/M^{-1} cm^{-1}): 275 (*Sh*); 325 (2470); 387 (*Sh*); 448 (760); 626 (155). Elemental analysis (%) Found: C 53.5, H 3.5. Calc. for $C_{24}H_{20}FeIOP$: C 53.5, H 3.7.

$[Fe(\eta^5\text{-}Cp)(CO)(PPh_2(C_6H_4COOH))I]$ **2**

Yield: 84% (489 mg; 0.84 mmol). Irradiation time: 3 h. Dark green crystalline powder. IR (KBr, cm^{-1}): ν(OH) 3530, ν(C-H aromatics) 3055, ν(C≡O) 1944, ν(C=O carboxylic acid) 1689, ν(C-C aromatics) 1674, 1442. ^1H NMR (DMSO-d_6, Me_4Si, δ/ppm): 8.06 (d, 2, $H_{3'}$); 7.62–7.43 (comp, 10, $H_{2'}$+H_2+H_3+H_4); 4.61 (s, 5, Cp). ^{13}C NMR (DMSO-d_6, Me4Si, δ/ppm): 220.90 (d, J_{CP} = 31.2, C≡O); 166.99 (COOH); 141.10 (d, $^1J_{CP}$ = 41, C1′); 134.69 (dd, J_{CP} = 16, 44, C1); 133.37 (dd, J_{CP} = 9, 18, C2); 133.12 (d, $^2J_{CP}$ = 9, C2′); 132.05 (C4′); 130.52 (C4); 128.90 (d, $^3J_{CP}$ = 9, C3′); 128.48 (d, $^3J_{CP}$ = 9, C3); 83.03 (Cp). ^{31}P NMR (DMSO-d_6, δ/ppm): 68.35 (s). UV–vis DMSO, λ_{max}/nm (ε/M^{-1} cm^{-1}): 274 (14555); 330 (*Sh*); 447 (830); 627 (175). Elemental analysis (%) Found: C 51.3, H 3.6. Calc. for $C_{25}H_{20}FeIO_3P$: C 51.5, H 3.6.

$[Fe(\eta^5\text{-}Cp)(CO)(P(Ph\text{-}p\text{-}F)_3)I]$ **3**

Yield: 64% (379 mg; 0.64 mmol). Irradiation time: 5 h. Microcrystalline green powder. Single crystals for X-ray diffraction studies were obtained by crystallization from dichloromethane/*n*-hexane solution. IR (KBr, cm^{-1}): ν(C-H aromatics) 3062, ν(C≡O) 1944, ν(C-C aromatics) 1581, 1496. ^1H NMR (DMSO-d_6, Me_4Si, δ/ppm): 7.52 (s, 6, H_3); 7.33 (s, 6, H_2); 4.65 (s, 5, Cp). ^{13}C NMR (DMSO-d_6, Me_4Si, δ/ppm): 220.20 (d, J_{CP} = 31.2, C≡O); 161.54 (d, $^1J_{CF}$ = 248, C4); 135.54 (t, J = 10, C3); 131.30 (d, $^1J_{CP}$ = 45, C1); 115.60 (dd, J = 11, 21, C2); 82.81 (Cp). ^{31}P NMR (DMSO-d_6, δ/ppm): 65.97 (s). UV–vis in DMSO, λ_{max}/nm (ε/M^{-1} cm^{-1}): 281 (*Sh*), 329 (*Sh*), 437 (830), 626 (159). Elemental analysis (%) Found: C 47.0, H 2.6. Calc. for $C_{24}H_{17}F_3FeIOP$: C 46.2, H 2.7.

2.4. General procedure for the synthesis of $[Fe(\eta^5\text{-}Cp)(CO)(PR_3)(C_7H_6N_2)]^+$ complexes **4**-**6**

To a stirred and degassed solution of complexes **1**–**3** (0.17 mmol for **5**, **6**; 0.30 mmol for **4**) in dry acetone (30 ml) was added $AgPF_6$ (0.25 mmol for **5**, **6**; 0.45 mmol for **4**). After 1 h 4-aminobenzonitrile (0.17 mmol for **5**, **6**; 0.30 mmol for **4**) was added and the reaction followed for 24 h at room temperature. The precipitates were separated by cannula-filtration and the solvent was evaporated under vacuum. The residue was twice recrystallized from dry acetone/*n*-hexane and dry THF/*n*-hexane.

$[Fe(\eta^5\text{-}Cp)(CO)(PPh_3)(C_7H_6N_2)][PF_6]$ **4**

Yield: 85% (172 mg; 0.26 mmol). Dark red crystalline. IR (KBr, cm^{-1}): ν(C-H aromatics) 3080, ν(N≡C) 2245, ν(C≡O) 1982, ν(C-C aromatics) 1620, 1512, 1435, ν(P-F) 840. ^1H NMR (DMSO-d_6, Me_4Si, δ/ppm): 7.61–7.53 (comp, 9, H_3+H_4); 7.40–7.32 (m, 6, H_2); 6.88 (d, 2, J_{HH} = 8.5, H_7); 6.45 (d, 2, J_{HH} = 8.5, H_8); 5.08 (s, 5, Cp). ^{13}C NMR (DMSO-d_6, Me_4Si, δ/ppm): 217.11 (d, J_{CP} = 45.4, C≡O); 153.99 (C5); 137.61 (C6); 134.03 (C7); 132.76 (d, $^2J_{CP}$ = 10, C2); 131.93 (d, $^1J_{CP}$ = 45, C1); 131.25 (C4); 129.23 (d, $^3J_{CP}$ = 10, C3); 112.92 (C8); 93.58 (C9); 85.10 (Cp). ^{31}P NMR (DMSO-d_6, δ/ppm): 66.84 (s); −144.19 (setp, J_{PF} = 712, PF_6). UV–Vis in DMSO, λ_{max}/nm (ε/M^{-1} cm^{-1}): 284 (21555); 321 (23250); 409 (900); 509 (*Sh*). Elemental analysis (%) Found: C 52.9, H 3.5, N 3.8. Calc. for $C_{31}H_{26}F_6FeN_2OP_2$: C 52.4, H 3.7, N 3.9.

$[Fe(\eta^5\text{-}Cp)(CO)(PPh_2(C_6H_4COOH))(C_7H_6N_2)][PF_6]$ **5**

Yield: 88% (107 mg; 0.15 mmol). Dark red crystalline. IR (KBr, cm^{-1}): ν(OH) 3530, ν(C-H aromatics) 2970, ν(N≡C) 2245, ν(C≡O) 1990, ν(C=O carboxylic acid) 1705, ν(C-C aromatics) 1697, 1604, 1411, ν(P-F) 840. ^{1}H NMR (DMSO-d_6, Me_4Si, δ/ppm): 13.39 (broad, 1, COOH); 8.07 (m, 2, $H_{3'}$); 7.75–7.34 (comp, 12, $H_{2'}$+H_2+H_3); 6.90 (d, 2, H_7); 6.45 (comp, 4, H_8+NH_2); 5.13 (s, 5, Cp). ^{13}C NMR (DMSO-d_6, Me_4Si, δ/ppm): 222.28 (C≡O); 166.66 (COOH); 154.06 (C5); 137.82 (C6); 134.12 (C7); 133.7 (d, $^1J_{CP}$ = 18, C1); 133.45 (C1′); 133.23 (C2′); 132.97 (d, $^2J_{CP}$ = 10, C2); 131.52 (C4′); 131.33 (C4); 129.82 (C3′); 129.44 (t, $^3J_{CP}$ = 10, C3); 112.95 (C8); 93.59 (C9); 85.26 (Cp). ^{31}P NMR (DMSO-d_6, δ/ppm): 68.87 (s); −144.20 (sept, $^2J_{CP}$ = 10, C2); 131.93 (d, $^1J_{CP}$ = 45, C1); 131.25 (C4); 129.23 (d, $^3J_{CP}$ = 10, C3); 112.92 (C8); 93.58 (C9); 85.10 (Cp). ^{31}P NMR (DMSO-d_6, δ/ppm): 66.84 (s); −144.19 (setp, J_{PF} = 712, PF_6). UV–Vis in DMSO, λ_{max}/nm (ε/M^{-1} cm^{-1}): 282 (38980); 319 (*Sh*); 410 (*Sh*); 510 (*Sh*). Elemental analysis (%) Found: C 46.9, H 3.5, N 3.3. Calc. for $C_{32}H_{26}F_6FeN_2O_3P_2 \cdot \frac{2}{5}AgI$: C 47.3, H 3.2, N 3.4.

[Fe(η^5-Cp)(CO)(P(Ph-p-F)$_3$)($C_7H_6N_2$)][PF_6] **6**

Yield: 88% (109 mg; 0.15 mmol). Dark red crystalline. IR (KBr, cm^{-1}): ν(C-H aromatics) 3078, ν(N≡C) 2252, ν(C≡O) 1990, ν(C-C aromatics) 1589, 1496, ν(P-F) 848. ^{1}H NMR (DMSO-d_6, Me_4Si, δ/ppm): 7.45–7.37 (comp, 12, H_2+H_3); 6.98 (d, 2, J_{HH} = 8.3, H_7); 6.48 (m, 4, H_8+NH_2); 5.13 (s, 5, Cp). ^{13}C NMR (DMSO-d_6, Me_4Si, δ/ppm): 216.84 (d, J_{CP} = 47.0, C≡O); 163.69 (d, $^1J_{CF}$ = 250, C4); 154.12 (C5); 137.84 (C6); 135.45 + 116.69 (C2+C3); 134.12 (C7); 128.03 (d, $^1J_{CP}$ = 51, C1); 112.98 (C8); 93.46 (C9); 85.26 (Cp). ^{31}P NMR (DMSO-d_6, δ/ppm): 68.87 (s); −144.20 (sept, $^2J_{CP}$ = 10, C2); 131.93 (d, $^1J_{CP}$ = 45, C1); 131.25 (C4); 129.23 (d, $^3J_{CP}$ = 10, C3); 112.92 (C8); 93.58 (C9); 85.10 (Cp). ^{31}P NMR (DMSO-d_6, δ/ppm): 66.84 (s); −144.19 (setp, J_{PF} = 712, PF_6). UV–vis in DMSO, λ_{max}/nm (ε/M^{-1} cm^{-1}): 284 (17248); 311 (18339); 406 (600). Elemental analysis (%) Found: C 49.8, H 3.4, N 3.0. Calc. for $C_{31}H_{23}F_9FeN_2OP_2 \cdot \frac{1}{2}CH_2Cl_2$: C 49.1, H 3.1, N 3.6.

2.5. X-ray crystal structure determination

Three-dimensional X-ray data for [Fe(η^5-Cp)(CO)(PPh_3)I] **1** and [Fe(η^5-Cp)(CO)(P(Ph-p-F)$_3$)I] **3** were collected on a Bruker SMART Apex CCD diffractometer at 100(2) K, using a graphite monochromator and Mo-K_α radiation (λ = 0.71073 Å) by the ϕ-ω scan method. Reflections were measured from a hemisphere of data collected of frames each covering 0.3° in ω. A total of 2892 reflections were measured, all of which were corrected for Lorentz and polarization effects and for absorption by semi-empirical methods based on symmetry-equivalent and repeated reflections. Of the total, 2687 independent reflections exceeded the significance level $|F|/\sigma(|F|) > 4.0$. After data collection, in each case a multi-scan absorption correction (SADABS) [26] was applied, and the structure was solved by direct methods and refined by full matrix least-squares on *F* [2] data using SHELX suite of programs [27]. The structure was solved by direct methods and refined by full-matrix least-squares methods on F^2. The non-hydrogen atoms were refined with anisotropic thermal parameters in all cases. Hydrogen atoms were included in calculation positions and refined in the riding mode. A final difference Fourier map showed a residual density outside due to disorder, which could not be refined: 2.303 and −1.542 e.Å^{-3}. A weighting scheme w = 1/[$\sigma^2(F_o^2)$ + (0.088000 P) [2] + 48.334400 P] for **1**, where P = ($|F_o|^2 + 2|F_c|^2$)/3, was used in the latter stages of refinement. CCDC No. 1536687 and 1565463 contains the supplementary crystallographic data for **1** and **3**, respectively. These data can be obtained free of charge via http://www.ccdc.cam.ac.uk/conts/retrieving.html, or from the Cambridge Crystallographic Data Centre, 12 Union Road, Cambridge CB2 1EZ, UK; fax: (+44) 1223-336-033; or e-mail: deposit@ccdc.cam.ac.uk. Crystal data and details of the data collection and refinement for the new compound were collected in Table 1.

2.6. Stability studies in DMSO and DMSO/DMEM

For the stability studies, all the complexes were dissolved in DMSO or 5% DMSO/95% DMEM at *ca.* 1 × 10^{-4} M and their electronic spectra were recorded in the range allowed by the solvents at set time intervals.

2.7. Biological studies

2.7.1. Cell lines and culture conditions

Human cervix adenocarcinoma HeLa cell line (ATC CCL-2) was maintained in a Minimum Essential Medium (MEM) alpha medium supplemented with 10% (v/v) heat inactivated fetal bovine serum (FBS) in a highly humidified atmosphere of 95% air with 5% CO_2 at 37 °C.

2.7.2. Cytotoxicity assays

Cells were seeded into a 96-well plate at a cell density of 3.0 × 10^3 cell/well and incubated for 24 h before the addition of the ligands or iron compounds a concentrations ranging from 0 to 200 μM. The growth inhibitory effect was measured after 24 and 72 h treatment by the XTT assay [28]. Aliquots of 20 μL of XTT solution [2,3-bis-(2-methoxy-4-nitro- 5-sulfophenyl)-2H-tetrazolium-5-carboxanilide] were added to each well. After 3 h, the colour formed was quantified by a spectrophotometric plate Reader (PerkinElmerVictor3 V) at 490 nm wavelength. Cell cytotoxicity was evaluated in terms of cell-growth inhibition in treated cultures and expressed as a % of the control conditions. Each experiment was repeated at least three times, and each concentration tested in at least six replicates.

2.7.3. In vitro apoptosis assay

Induction of apoptosis *in vitro* by iron compounds was determined by a flow cytometric assay with Annexin V-FITC by using an Annexin V-FITC Apoptosis Detection Kit (Roche). Exponentially growing HeLa cells in 6-well plates (4 × 10^5 cells per well) were exposed to concentrations equal to the IC_{50} of the iron compounds for 24 h or cisplatin as a reference. Cells were collected, washed with PBS, and resuspended in 100 μL of binding buffer. Annexin V staining was accomplished following the product instruction (Roche). In brief, 2 μL of Annexin V-fluorescein isothiocyanate (FITC) and 2 μL of propidium iodide (PI) were added to the samples for 15 min at room temperature in the dark. The amount of apoptotic cells was analysed by flow cytometry (FACSCalibur, Becton Dickinson).

3. Results and discussion

3.1. Synthesis

New iron(II) organometallic compounds have been synthesized. The neutral compounds [FeCp(CO)(PR_3)I] (where PR_3 = triphenylphosphane **1**, 4-(diphenylphosphino)benzoic acid **2** or tris(4-fluorophenyl)phosphane **3**) have been synthesized by UV irradiation of a solution of [Fe(Cp)$(CO)_2$I] and the corresponding phosphane ligand in acetone (Scheme 1). The cationic compounds [Fe(Cp)(CO)(PR_3)(4-aminobenzonitrile)]$^+$ (where PR_3 = triphenylphosphane **4**, 4-(diphenylphosphino)benzoic acid **5** or tris(4-fluorophenyl)phosphane **6**) were obtained by iodide abstraction using $AgPF_6$ and reaction with 4-aminobenzonitrile in acetone at room temperature for 24 h (Scheme 1). All the compounds were obtained in good yields (64–88%) as dark green

Table 1
Crystal data and structure refinement for [Fe(η^5-Cp)(CO)(PPh_3)I] **1** and for [Fe(η^5-Cp)(CO)(P(Ph-p-F)$_3$)I] **3**.

	1	3
Formula	$C_{24}H_{20}FeIOP$	$C_{24}H_{17}F_3FeIOP$
Formula weight	538.12	592.10
T, *K*	100(2)	100(2)
Wavelength, Å	0.71073	0.71073
Crystal system	Orthorhombic	Orthorhombic
Space group	$P2_12_12_1$	*Pbca*
a/Å	8.6776(6)	15.4421(5)
b/Å	13.6856(9)	16.5176(6)
c/Å	17.1867(11)	16.7701(6)
V/Å^3	2041.1(2)	4277.5(3)
Z	4	8
F_{000}	1064	2320
D_{calc}/g cm^{-3}	1.751	1.839
μ/mm^{-1}	2.342	2.264
θ/(°)	1.90 to 28.34	2.18 to 26.42
R_{int}	0.0535	0.0705
Absolute structure parameter (Flack parameter)	0.08(11)	
Crystal size/mm^3	0.14 × 0.13 × 0.13	0.124 × 0.090 × 0.085
Goodness-of-fit on F^2	1.132	1.329
R_1 [a]	0.0799	0.1031
wR_2 (all data) [b]	0.2222	0.2080
Largest differences peak and hole (eÅ^{-3})	2.303 and −1.542	2.213 and −1.977

[a] $R_1 = \Sigma||F_o| - |F_c||/\Sigma|F_o|$.
[b] $wR_2 = \{\Sigma[w(|F_o|^2 - |F_c|^2|)^2]/\Sigma[w(F_o^2)^2]\}^{1/2}$.

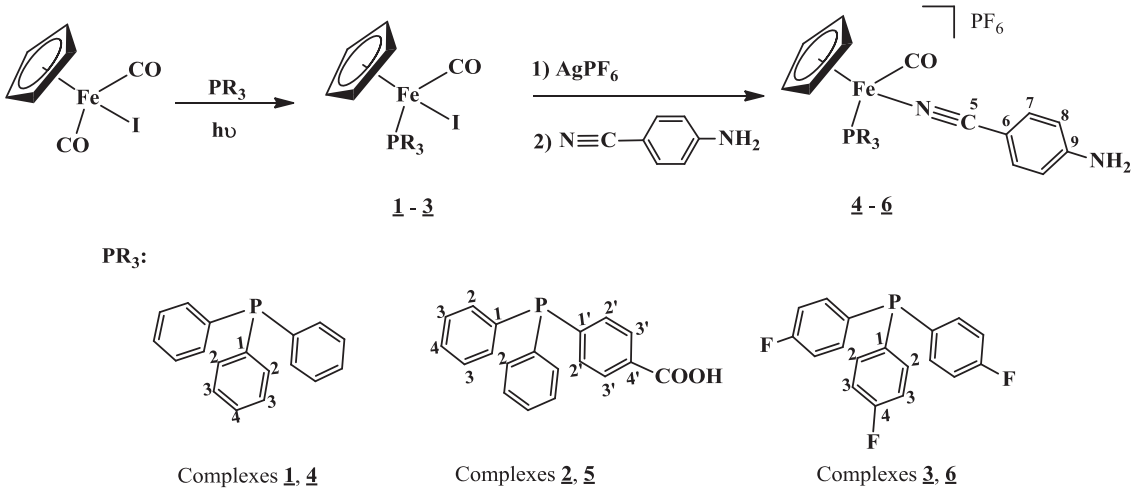

Scheme 1. Reaction scheme for compounds **1**–**6**, numbered for NMR purposes.

(complexes **1**–**3**) or dark red compounds (complexes **4**–**6**). The formulation and purity of all the new compounds has been ascertained by elemental analysis and FT-IR and multinuclear (^{1}H, ^{13}C and ^{31}P) NMR spectroscopy. Compound **1** has been previously reported [29]. In this paper from 1966, the reaction was carried out in benzene at reflux temperature for 18 h. During the reaction two products were formed, being [FeCp(CO)(PPh_3)I] isolated in ~34% yield and only characterized by FT-IR and elemental analysis. Later, a different synthesis approach was suggested [30], based on a paper describing the synthesis of iron cyclopentadienyl complexes with triphenylphosphite ligands [31] using UV irradiation in cyclohexane, benzene or THF. However, neither synthesis details nor characterization is provided. Here, we present an improved synthesis (69% yield) based on those papers, together with a complete spectroscopic characterization and the X-ray structure of **1** (see below).

The solid state FT-IR spectra (KBr pellets) of all the complexes present the characteristic band for the cyclopentadienyl ring along with the aromatic rings of the phosphane ligands (3200-3000 cm^{-1} and 1600-1400 cm^{-1}). Additional bands at ~850 cm^{-1} confirm the presence of the counter-ion PF_6^- for compounds **4**–**6**. The presence of carbon monoxide can be confirmed by the infrared stretching vibration occurring at *ca.* 1940 cm^{-1} in compounds **1**–**3** and at *ca.* 1990 cm^{-1} in compounds **4**–**6**. These vibrations in compounds **1**–**3** are present at lower values than those of the parent dicarbonyl compound [FeCp(CO)$_2$I] (ν = 2037 and 1975 cm^{-1}). These differences are consistent with the enhancement of bonding between the metal and the remaining terminal carbonyl group, due to the replacement of one CO in [FeCp(CO)$_2$I] by the poorer π-acceptor phosphane. The replacement of the iodide by the nitrile ligand in compounds **4**–**6** leads to a strengthening of the CO bond and accounts for the competition effect of the metal–ligand π-back-donation. The coordination of the 4-aminobenzonitrile in compounds **4**–**6** can be also confirmed by the characteristic stretching vibration of the nitrile functional group appearing at 2214 cm^{-1} in the free ligand and at ~2247 cm^{-1} after coordination.

Table 2
NMR assignments for compounds **1**–**6**, phosphanes and 4-aminobenzonitrile in DMSO-d_6.

	^{1}H NMR			^{31}P NMR
	Cp	H_7	H_8	PR_3
Triphenylphosphane PPh_3	–	–	–	−7.0
4-(diphenylphosphino)benzoic acid $PPh_2(C_6H_4COOH)$	–	–	–	−6.5
tris(4-fluorophenyl)phosphane $P(Ph\text{-}p\text{-}F)_3$	–	–	–	−10.6
4-aminobenzonitrile	–	7.35	6.60	–
1	4.59	–	–	67.04
2	4.61	–	–	68.35
3	4.65	–	–	65.97
4	5.10	6.88	6.45	66.84
5	5.17	6.90	6.45	67.48
6	5.13	6.98	6.47	65.87

This variation of ~30 cm^{-1} for $\nu_{N\equiv C}$ accounts for the σ coordination and the effect of metal–ligand π-backdonation through d_{metal}–π^*_{ligand} interaction which was as also observed in other related compounds [30].

The NMR spectra in DMSO-d_6 shows the expected signals of the Cp ligand at ~4.6 ppm for compounds **1**–**3** and at ~5.1 ppm for compounds **4**–**6**, more deshielded in this later case due to their cationic nature (Table 2). The replacement of one CO strong π-acceptor ligand in the parent complex $[Fe(Cp)(CO)_2I]$, by a more electron donating phosphane ligand is accompanied by a shielding on the Cp (5.28 *vs*. ~4.6 ppm), owing to the increased electron density at the metal centre. This donation effect of the phosphane is in agreement with the phosphane deshielding observed on the ^{31}P NMR sharp singlet resonance upon coordination (Table 2). The ^{1}H NMR signals of the 4-aminobenzonitrile are shielded in all the cationic complexes **4**–**6**, being this effect more pronounced in the *ortho* protons ($\Delta\delta = -0.37$ to -0.47 ppm), in agreement with an electronic flow from the metal centre to the nitrile functional group due to the effect of π-backdonation. Accordingly, an increased electronic density is observed on the 4-aminobenzonitrile aromatic ring. The ^{13}C NMR spectra shows the same general effect observed for the protons in all complexes.

3.2. UV–visible (UV–Vis) studies

3.2.1. Compounds characterization

The electronic absorption spectra of all compounds was recorded in 1×10^{-3} to 1×10^{-5} M solutions in dimethyl sulfoxide in the wavelength range of 268–900 nm. The electronic data is summarized in the experimental section and in Fig. 1.

The spectra are characterized by a strong absorption band below 285 nm and a shoulder at around 320–330 nm. The first is attributed to $\pi \rightarrow \pi^*$ transitions on the chromophores (phosphanes and also nitrile for **4**–**6**). The latter is attributed to electronic transitions occurring in the organometallic fragment $\{FeCp\}^+$ (by analogy with the iron parental complex $[Fe(Cp)(CO)_2I]$, Fig. S1). These bands are much more intense in the cationic compounds. In addition, one or two weak bands in the visible region were found for all complexes. The first one ($600\ M^{-1}cm^{-1} < \varepsilon < 850\ M^{-1}cm^{-1}$) is probably due to metal-to-ligand charge transfer bands (MLCT), since ^{1}H NMR and FT-IR studies showed the presence of π-backdonation from the metal centre to the nitrile and to the carbonyl, as also observed for other related compounds [30]. The second band in the visible range, with molar absorptivity values below 200 $M^{-1}cm^{-1}$ might be due to DMSO-d_6 iron transitions.

3.2.2. Complexes stability

Envisaging the use of these new compounds as cytotoxic agents and their study in human cancer cell lines, their stability and behaviour was studied in DMSO (co-solvent used in the biological assays) and in culture cellular media (DMEM), using 5% DMSO. All the compounds are fairly stable in both solutions for a period of at least 24 h as one can observe by UV–Vis (Figs. S2 and S3 in Supporting Information) or NMR spectroscopy (in DMSO-d_6, Fig. S4),

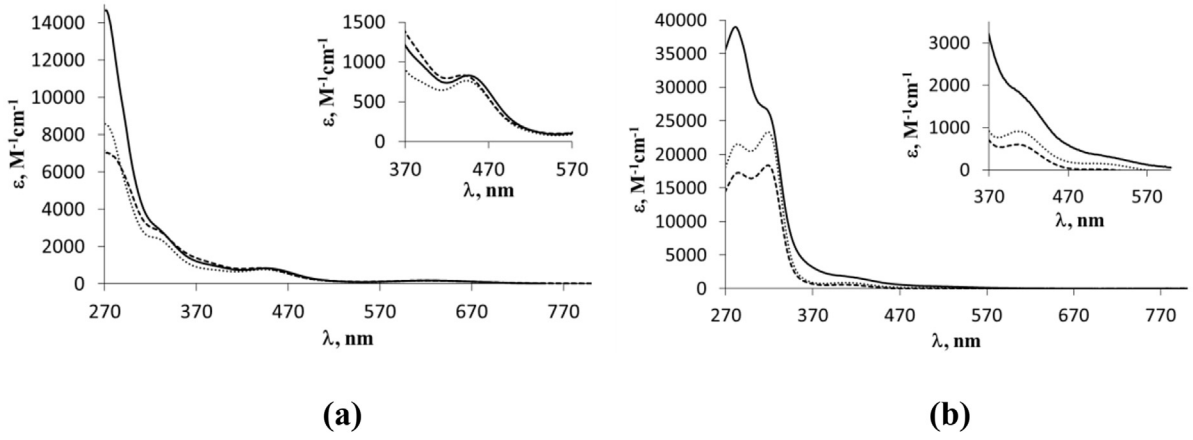

Fig. 1. Electronic spectra of the new iron compounds in DMSO solutions.

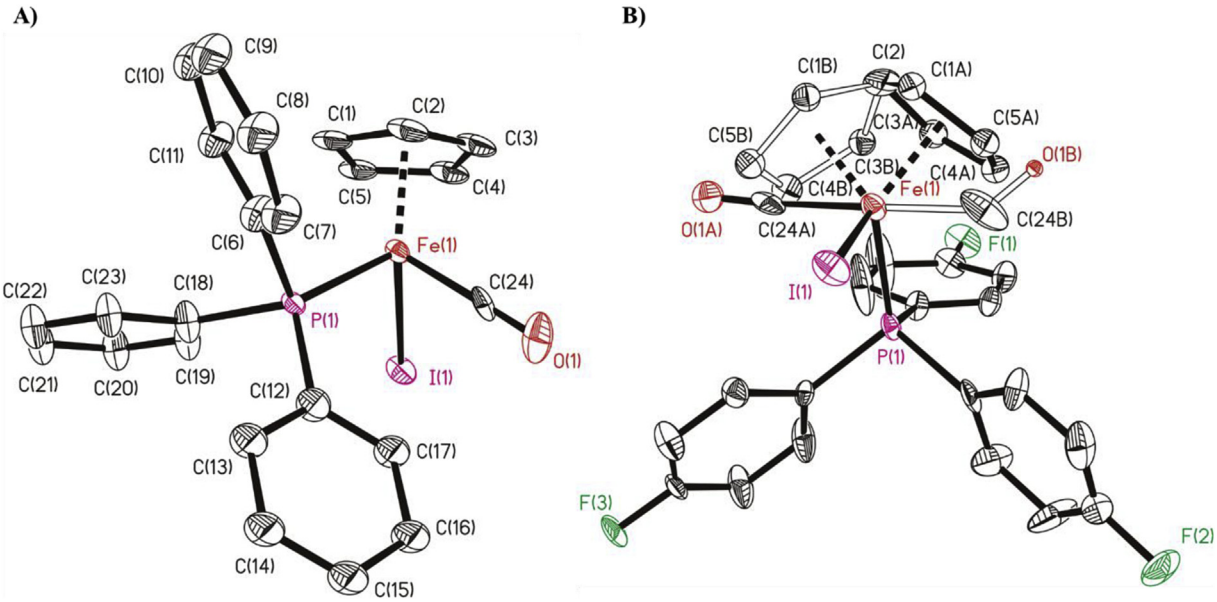

Fig. 2. ORTEP plot for the complex **A)** [Fe(η^5-Cp)(CO)(PPh_3)I] **1** and **B)** [Fe(η^5-Cp)(CO)(P(Ph-p-F)$_3$)I] **3**. All the non-hydrogen atoms are presented by their 50% probability ellipsoids. Hydrogen atoms are omitted for clarity.

since no changes in band format or the appearance of new bands was noticed.

3.3. *Single crystal structure of [Fe(η^5-Cp)(CO)(PPh_3)I] **1** and [Fe(η^5-Cp)(CO)(P(Ph-p-F)$_3$)I] **3***

[Fe(η^5-Cp)(CO)(PPh_3)I] **1** crystallizes from THF/*n*-hexane solution as red blocks (crystal dimensions 0.14 × 0.13 × 0.13 mm). Fig. 2A shows an ORTEP representation of [Fe(η^5-Cp)(CO)(PPh_3)I] of **1**. The compound crystallizes in a non-centrosymmetric space group, $P2_12_12_1$. Crystal packing only contains one enantiomer of iron complex due to short contacts and π-π angular interactions, which prevent the free rotoinversion around Fe-I edge. Short contacts are observed between phenyl rings and oxygen atoms of CO molecules in compound **1** (see Fig. 3). The distance between O(1)-C(10) is 2.862(13) Å and between O(1)-C(11) is 2.495(14) Å (through symmetry operation, 1-x,-1/2 + y,1.5-z). The result is the presence of dimeric structures in the crystal packing. Weak π-π angular interactions are observed between Cp and Ph rings in these dimeric moieties. The rings are not parallel. The distance between centroids, $d_{c1\text{-}c2}$, is 3.958(16) Å [c1, C(12A)-C(13A)-C(14A)-C(15A)-C(16A)-C(17A), c2, C(1K)-C(2K)-C(3K)-C(4K)-C(5K)]. The obtained Flack parameter (see Table 1) corresponds with an enantiomerically pure compound [32].

[Fe(η^5-Cp)(CO)(P(Ph-p-F)$_3$)I] **3** crystallizes from dichloromethane/*n*-hexane solution as black blocks (crystal dimensions 0.124 × 0.090 × 0.085 mm). Fig. 2B shows an ORTEP representation of **3**. The compound crystallizes in a centrosymmetric space group, *Pbca*. Short contacts and π-π interactions are not present in the crystal packing of this structure (see Fig. 4). The compound presents an important disorder in the structure, which can be justified for the presence of the two enatiomers in the crystal packing.

In the molecular structures, the ruthenium centres adopt a "piano stool" distribution formed by the iron-Cp unit bound to one phosphane, one CO molecule and one iodide anion. The C-O bond length, 1.071(17) Å in **1** and 1.07(2) Å in **3**, is shorter than in other

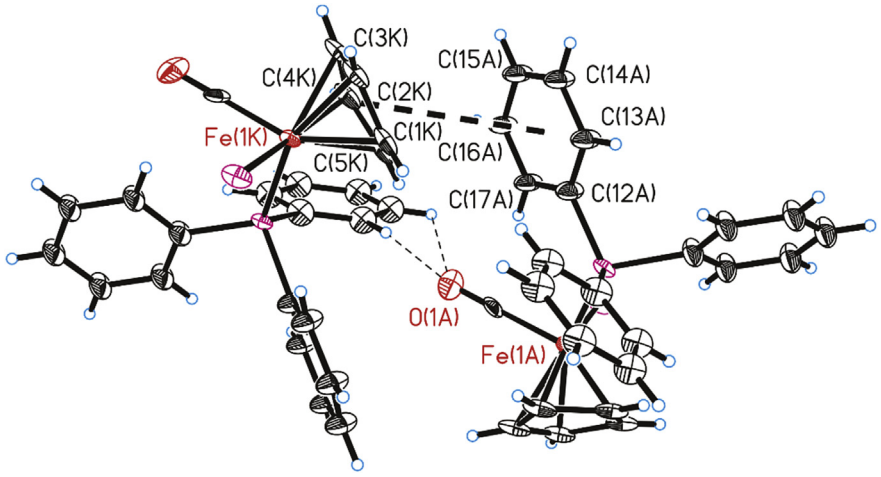

Fig. 3. Dimeric structures present in the crystal packing of [Fe(η^5-Cp)(CO)(PPh_3)I] **1**. π-π angular interactions between phenyl and Cp groups are showed by thick dashed black lines. Short contacts between CO molecules and phenyl groups are showed by fine dashed black lines.

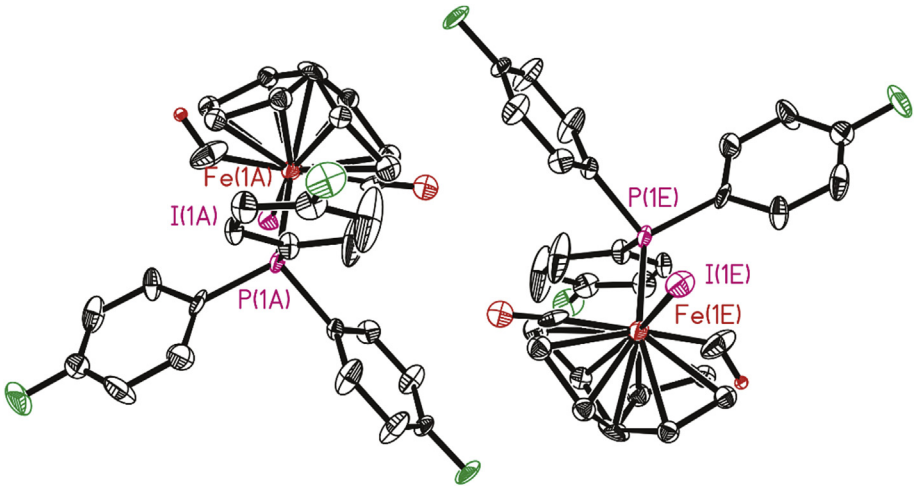

Fig. 4. Partial section in the crystal packing of [Fe(η^5-Cp)(CO)(P(Ph-p-F)$_3$)I] **3**.

compounds, where the Fe back-bonding into the CO π^* orbital is more important [33]. The Fe-C bond length is determined predominantly by the steric constraints of the phosphane ligand rather than being a consequence of the bond. The distance between Fe and the centroid of the π-bonded cyclopentadienyl moiety is 1.669(15) Å to Fe centre in **1** (ring slippage 0.026 Å) and 1.7403(16) Å for unit A and 1.6793(17) Å for unit B in **3** (ring slippage, 0.077 Å and 0.088 Å, respectively). The mean value of the Fe-C bond distance is 2.072(14) Å in **1** and 2.123(18) Å for unit A and 2.110(3) Å for unit B, in **3**. Table 3 contains selected bond lengths and angles for the two compounds.

3.4. Cytotoxicity of the iron complexes against HeLa cells

The cytotoxic effect of the iron complexes (**1**–**6**) was examined on human cervical cancer cells (HeLa) using the XTT assay, a colorimetric determination of cell viability during *in vitro* treatment with a drug. Cells were exposed to each compound (Fe(II) complexes, and all the ligands) continuously for a 24 or 72 h period and then assayed for growth using the XTT end point assay. The IC_{50} values of iron complexes for the growth inhibition of Hela cells are summarized in Table 4 and the IC_{50} curves can be found in Supporting Information (Fig. S5). Among the ligands, only tris(4-fluorophenyl)phosphane showed some cytotoxicity at 72 h with an IC_{50} of 60.81 ± 3.43 μM (ligands IC_{50} is presented in Supporting Information). None of the neutral compounds **1**–**3** was cytotoxic in this cell line. Relatively to the cationic compounds **4**–**6**, one can observe the effect of the phosphane ligand on the overall cytotoxicity. Compound **5** bearing 4-(diphenylphosphino)benzoic acid is non-cytotoxic, while the compounds bearing tris(4-fluorophenyl) phosphane **6** and triphenylphosphane **4** were found to be quite cytotoxic against HeLa cells (in the micromolar range) being the cytotoxicity dependent on the exposition time. These values are in the same range for those obtained for $[Fe(Cp)(dppe)(L)]^+$ compounds (dppe = ethylenebis(diphenylphosphane); L = imidazole based ligands) [19] and for $[Fe(Cp)(CO)_2X]$ (X = halide, NCS, BF_4^-) [22]. Noteworthy, comparing with the latter example, the replacement of one CO ligand in $[Fe(Cp)(CO)_2I]$[22] by a phosphane $[Fe(Cp)(CO)(PR_3)I]$ (**1**–**3**) led to a sharp decrease (6.7 ± 1.1 *vs.* > 200 μM at 24 h incubation) on the compounds cytotoxicity emphasizing the importance of the compounds electronic features. Substitution of iodine by a second π acceptor ligand such as 4-aminobenzonitrile, $[Fe(Cp)(CO)(PR_3)(C_7H_6N_2)]$ (**4** and **6**) leads to the reestablishment of the cytotoxicity with IC_{50} of 3.76 and 4.92 μM, for **4** and **6**, respectively, at 72 incubation. These values are better than those of cisplatin (7.0 ± 2.70) in the same conditions [19]. The relation between the electronic flow throughout the compounds creating an asymmetric charge density in the molecule and their cytotoxicity has been already established for some ruthenium-cyclopentadienyl families of compounds [16,17]. The lack of activity in the case of compound **5** bearing the 4-(diphenylphosphino)benzoic acid seems to be related to the substituent group on the phosphane ligand. One could postulate that the carboxylic acid group might be negatively charged in the cellular media, which may well hinder its cellular uptake [34].

Table 3
Bond lengths [Å] and angles [°] for [Fe(η^5-Cp)(CO)(PPh$_3$)I] **1** and [Fe(η^5-Cp)(CO)(P(Ph-p-F)$_3$)I] **3**.

Bond lengths	1	3
Fe(1)-I(1)	2.6218(16)	2.6226(17)
Fe(1)-C(2)	2.043(14)	2.108(12)
Fe(1)-P(1)	2.227(3)	2.209(3)
		A atoms B atoms
Fe(1)-C(1)	2.068(15)	2.123(17) 2.06(3)
Fe(1)-C(3)	2.104(12)	2.075(18) 2.05(3)
Fe(1)-C(4)	2.083(14)	2.137(18) 2.20(4)
Fe(1)-C(5)	2.064(15)	2.173(17) 2.13(4)
Fe(1)-C(24)	1.806(14)	1.775(19) 1.78(3)
O(1)-C(24)	1.071(17)	1.07(2) 1.07(3)
Bond angles	**1**	**3**
C(2)-Fe(1)-P(1)	98.8(4)	137.4(3)
		A atoms B atoms
C(24)-Fe(1)-P(1)	93.2(4)	92.9(6) 83.7(13)
C(5)-Fe(1)-P(1)	114.6(5)	118.0(4) 111.2(8)
C(1)-Fe(1)-P(1)	88.8(4)	155.8(4) 151.5(8)
C(4)-Fe(1)-P(1)	156.3(5)	92.1(5) 83.9(10)
C(3)-Fe(1)-P(1)	136.9(4)	100.7(4) 97.4(7)

3.5. Determination of cell death mechanism by Annexin V/PI assay

The cell death mechanism was evaluated by Annexin V/PI flow cytometry for the two cytotoxic compounds **4** and **6**. HeLa cells were incubated at equitoxic concentrations (IC_{50} values) during 24 h and cisplatin was used as a reference. Annexin V binds phosphatidyl serine residues, which are asymmetrically distributed toward the inner plasma membrane but migrate to the outer plasma membrane during apoptosis. As can be seen in Table 5, both complexes, **4** and **6**, induce apoptosis in great extent, comparable to

Table 4
IC_{50} values (μM) of iron compounds (**1**–**6**), $[Fe(Cp)(dppe)(L)]^+$ (dppe = ethylenebis(diphenylphosphane); L = imidazole based ligands), $[Fe(Cp)(CO)_2X]$ (X = halide, NCS, BF_4^-), $[Ru(Cp)(PPh_3)_2$(clotrinazole)]+ and cisplatin against HeLa cells.

Complex	IC $_{50}$ (μM) 24 h	IC_{50} (μM) 72 h
1	>200	>200
2	>200	>100
3	>200	>200
4	18.97 ± 1.95	3.76 ± 1.07
5	>200	>100
6	18.44 ± 2.14	4.92 ± 1.25
$[Fe(Cp)(dppe)(L)]^+$	–	1.4 ± 0.35–6.3 ± 1.10[19]
$[Fe(Cp)(CO)_2X]$	6.7 ± 1.1–18.3 ± 1.2[22]	–
$[Ru(Cp)(PPh_3)_2$(clotrinazole)$]^+$	–	3.6 ± 1.1[35]
Cisplatin	–	7.0 ± 2.70[19]

Table 5
Percentage of HeLa cells in each state after treatment with complexes **4**, **6** and Cisplatin at IC_{50} concentration for 24 h of incubation.

	% vital cells (R1)	*% apoptotic cells (R2)*	*% late apoptosis or dead cells (R3)*	*% damaged cells (R4)*
Control	90.52	4.67	3.25	1.57
Cisplatin	62.19	23.85	13.43	0.53
4	57.60	24.63	16.64	1.12
6	67.28	18.25	13.05	1.42

the values found for cisplatin and correlating well with the cytotoxicity assays. This is a highly desirable feature for a drug candidate since apoptosis is a controlled mechanism of cell death.

4. Conclusion

A new family of Fe(II) compounds based on the general structure $[Fe(Cp)(CO)(PR_3)(L)]^n$ (PR_3 = triphenylphosphane, 4-(diphenylphosphino)benzoic acid or tris(4-fluorophenyl)phosphane; when L = I, n = 0; when L = 4-aminobenzonitrile, n = +1) has been successfully synthesized and characterized. Compound $[Fe(Cp)(CO)(PPh_3)I]$ **1** crystalizes in the orthorhombic space group $P2_12_12_1$, while compound $[Fe(\eta^5\text{-}Cp)(CO)(P(Ph\text{-}p\text{-}F)_3)I]$ **3** crystalizes in the centrosymmetric space group *Pbca*. In both cases the iron centre adopts the expected "piano stool" structure.

The cationic compounds **4** and **6** were found to be cytotoxic against cervical human cancer cells (HeLa) in the micromolar range, inducing cell death by apoptosis within the same range as cisplatin. Structural features observed on our spectroscopic data point out that the asymmetric charge distribution created by the electronic flow through the complexes might be related to their cytotoxic activity. This effect can be explained by an enhancement of the interaction of the compounds with the negatively charged cancer cell membranes, disrupting the negative potential of cell membranes. Importantly, compounds **4** and **6** present similar activity to others Ru-Cp related compounds for HeLa cell line at the same time of incubation [35]. This pinpoint that FeCp compounds, based on bio essential and less expensive metal (relatively to others commonly used in the search of metallodrugs), deserve more detailed studies to unravel their mechanism of action.

Acknowledgements

This work was financed by the Portuguese Foundation for Science and Technology (Fundação para a Ciência e Tecnologia, FCT) within the scope of project UID/QUI/00100/2013. Andreia Valente and Adhan Pilon acknowledge the Investigator FCT2013 Initiative for the project IF/01302/2013 (acknowledging FCT, as well as POPH and FSE - European Social Fund). Julia Lorenzo acknowledge funding from the Spanish Ministry of Economy Industry and Competitiveness contract BIO2016-78057-R.

Appendix A. Supplementary data

Supplementary data related to this article can be found at https://doi.org/10.1016/j.jorganchem.2017.10.004.

References

[1] S.V. Torti, F.M. Torti, Nat. Rev. Cancer 13 (2013) 342–355.
[2] T.J. Kealy, P.L. Pauson, Nature 168 (1951) 1039–1040.
[3] G. Wilkinson, M. Rosenblum, M.C. Whiting, R.B. Woodward, J. Am. Chem. Soc. 74 (1952) 2125–2126.
[4] P. Köpf-Maier, H. Köpf, E.W. Neuse, Angew. Chem. Int. Ed. Engl. 23 (1984) 456–457.
[5] P. Köpf-Maier, H. Köpf, E.W. Neuse, J. Cancer Res. Clin. Oncol. 108 (1984) 336–340.
[6] S.S. Braga, A.M.S. Silva, Organometallics 32 (2013) 5626–5639.
[7] G. Gasser, I. Ott, N. Metzler-Nolte, J. Med. Chem. 54 (2011) 3–25.
[8] M.J. Scandlyn, E.C. Stuart, T.J. Somers-Edgar, A.R. Menzies, R.J. Rosengren, Br. J. Cancer 99 (2008) 1056–1063.
[9] H. Seeger, J. Huober, D. Wallwiener, A.O. Mueck, Horm. Metab. Res. 36 (2004) 277–280.
[10] M. Murty, Can. J. Physiol. Pharmacol. 85 (2007) 952–955.
[11] T.S. Morais, F.C. Santos, T.F. Jorge, L. Côrte-Real, P.J.A. Madeira, F. Marques, M.P. Robalo, A. Matos, I. Santos, M.H. Garcia, J. Inorg. Biochem. 130 (2014) 1–14.
[12] V. Moreno, M. Font-Bardia, T. Calvet, J. Lorenzo, F.X. Avilés, M.H. Garcia, T.S. Morais, A. Valente, M.P. Robalo, J. Inorg. Biochem. 105 (2011) 241–249.
[13] M. Helena Garcia, T.S. Morais, P. Florindo, M.F.M. Piedade, V. Moreno, C. Ciudad, V. Noe, J. Inorg. Biochem. 103 (2009) 354–361.
[14] A.I. Tomaz, T. Jakusch, T.S. Morais, F. Marques, R.F.M. de Almeida, F. Mendes, E.A. Enyedy, I. Santos, J.C. Pessoa, T. Kiss, M.H. Garcia, J. Inorg. Biochem. 117 (2012) 261–269.
[15] A. Valente, M.H. Garcia, F. Marques, Y. Miao, C. Rousseau, P. Zinck, J. Inorg. Biochem. 127 (2013) 79–81.
[16] L. Côrte-Real, M. Paula Robalo, F. Marques, G. Nogueira, F. Avecilla, T.J.L. Silva, F.C. Santos, A. Isabel Tomaz, M. Helena Garcia, A. Valente, J. Inorg. Biochem. 150 (2015) 148–159.
[17] T.S. Morais, A. Valente, A.I. Tomaz, F. Marques, M.H. Garcia, Future Med. Chem. 8 (2016) 527–544.
[18] N. Mendes, F. Tortosa, A. Valente, F. Marques, A. Matos, T.S. Morais, A.I. Tomaz, F. Gärtner, M.H. Garcia, Anticancer. Agents Med. Chem. 17 (2017) 126–136.
[19] A.C. Gonçalves, T.S. Morais, M.P. Robalo, F. Marques, F. Avecilla, C.P. Matos, I. Santos, A.I. Tomaz, M.H. Garcia, J. Inorg. Biochem. 129 (2013) 1–8.
[20] A. Valente, A.M. Santos, L. Côrte-Real, M.P. Robalo, V. Moreno, M. Font-Bardia, T. Calvet, J. Lorenzo, M.H. Garcia, J. Organomet. Chem. 756 (2014) 52–60.

[21] P.R. Florindo, D.M. Pereira, P.M. Borralho, C.M.P. Rodrigues, M.F.M. Piedade, A.C. Fernandes, J. Med. Chem. 58 (2015) 4339–4347.
[22] H.T. Poh, P.C. Ho, W.Y. Fan, RSC Adv. 6 (2016) 18814–18823.
[23] M.H. Garcia, M.P. Robalo, a R. Dias, M. Fa, J. Organomet. Chem. 619 (2001) 252–264.
[24] W.L.F. Armarego, C.L.L. Chai, Purif. Lab. Chem. (2009) 61–79.
[25] T.S. Piper, G. Wilkinson, J. Inorg. Nucl. Chem. 2 (1956) 38–45.
[26] G.M. Sheldrick, SADABS, Version 2.10, University of Göttingen, Germany, 2004.
[27] G.M. Sheldrick, Acta Crystallogr. Sect. A A64 (2008) 112–122.
[28] A. Cory, T. Owen, J. Barltrop, J. Cory, Cancer Commun. 3 (1991) 207–212.
[29] P.M. Treichel, R.L. Shubkin, K.W. Barnett, D. Reichard, Inorg. Chem. 5 (1966) 1177–1181.
[30] M.H. Garcia, M.P. Robalo, A.P.S. Teixeira, A.R. Dias, M.F.M. Piedade, M.T. Duarte, J. Organomet. Chem. 632 (2001) 145–156.
[31] A.N. Nesmeyanov, Y.A. Chapovskey, Y.A. Ustynyuk, J. Organomet. Chem. 9 (1967) 345–353.
[32] H.D. Flack, G. Bernardinelli, Chirality 20 (2008) 681–690.
[33] L. Mercs, G. Labat, A. Neels, A. Ehlers, M. Albrecht, Organometallics 25 (2006) 5648–5656.
[34] E. Fröhlich, Int. J. Nanomedicine 7 (2012) 5577–5591.
[35] E. Rodríguez Arce, C. Sarniguet, T.S. Moraes, M. Vieites, A.I. Tomaz, A. Medeiros, M.A. Comini, J. Varela, H. Cerecetto, M. González, F. Marques, M.H. García, L. Otero, D. Gambino, J. Coord. Chem. 68 (2015) 2923–2937.